Developmental Biology 458 (2020) 32–42

Contents lists available at ScienceDirect

Developmental Biology

journal homepage: www.elsevier.com/locate/developmentalbiology

Slit neuronal secretion coordinates optic lobe morphogenesis in *Drosophila*

Lorena Caipo [a,b], M. Constanza González-Ramírez [a], Pablo Guzmán-Palma [a], Esteban G. Contreras [b], Tomás Palominos [a], Nicolás Fuenzalida-Uribe [a], Bassem A. Hassan [c], Jorge M. Campusano [a], Jimena Sierralta [b], Carlos Oliva [a,*]

[a] Department of Cellular and Molecular Biology, Faculty of Biological Sciences, Pontificia Universidad Católica de Chile, Av Libertador Bernardo O'Higgins 340, Santiago, Chile
[b] Department of Neuroscience and Biomedical Neuroscience Institute, Faculty of Medicine, Universidad de Chile, Independencia 1027, Santiago, Chile
[c] Institut du Cerveau et de la Moelle Epinière (ICM) - Sorbonne Université, Hôpital Pitié-Salpêtrière, Inserm, CNRS, Paris, France

A B S T R A C T

The complexity of the nervous system requires the coordination of multiple cellular processes during development. Among them, we find boundary formation, axon guidance, cell migration and cell segregation. Understanding how different cell populations such as glial cells, developing neurons and neural stem cells contribute to the formation of boundaries and morphogenesis in the nervous system is a critical question in neurobiology. Slit is an evolutionary conserved protein essential for the development of the nervous system. For signaling, Slit has to bind to its cognate receptor Robo, a single-pass transmembrane protein. Although the Slit/Robo signaling pathway is well known for its involvement in axon guidance, it has also been associated to boundary formation in the *Drosophila* visual system. In the optic lobe, Slit is expressed in glial cells, positioned at the boundaries between developing neuropils, and in neurons of the medulla ganglia. Although it has been assumed that glial cells provide Slit to the system, the contribution of the neuronal expression has not been tested. Here, we show that, contrary to what was previously thought, Slit protein provided by medulla neurons is also required for boundary formation and morphogenesis of the optic lobe. Furthermore, tissue specific rescue using modified versions of Slit demonstrates that this protein acts at long range and does not require processing by extracellular proteases. Our data shed new light on our understanding of the cellular mechanisms involved in Slit function in the fly visual system morphogenesis.

1. Introduction

Secreted factors contribute to shaping the nervous system during development via the regulation of several cellular processes (Chilton, 2006; Yam and Charron, 2013; Zou, 2004). Cell migration, cell intercalation, boundary formation and axonal/dendrite pathfinding are highly controlled processes that govern morphogenesis (Walck-Shannon and Hardin, 2014; Cooper, 2013; Kiecker and Lumsden, 2005). Although these processes are generally studied separately, the molecules involved are shared in different contexts. For instance morphogens, molecules classically regarded as controlling cell fate in a concentration dependent manner, also regulate axon guidance (Chilton, 2006; Yam and Charron, 2013; Zou, 2004), while classic axon guidance factors can control cell migration and cell intercalation during boundary formation (Branda and Stern, 1999; Brose and Tessier-Lavigne, 2000; Hebrok and Reichardt, 2004; Tsai and Miller, 2002; Kemp et al., 2009). Strategies to identify the function of guidance cues involve expression pattern analyses and functional studies. However, recent literature has shown that it is essential to determine which cell population is, in each context, the relevant source of signaling molecules. A remarkable example of this is the discovery that Netrin, a member of a family of secreted guidance molecules, does not work only through secretion from the neural tube floor plate to generate a concentration gradient that control axon guidance, as previously thought (Kennedy et al., 1994, 2006). Instead, axons use Netrin presented by radial glial cell projections as short range cue to travel through haptotaxis, in a cell-cell contact dependent manner (Varadarajan et al., 2017; Dominici et al., 2017), and use floor plate derived Netrin as long range cue to find their way in the developing nervous system (Moreno-Bravo et al., 2019; Wu et al., 2019). This mechanism is in agreement with recent observations in the fly visual system (Timofeev et al., 2012; Akin and Zipursky, 2016).

The Slit ligand and its receptors Robo1, Robo2 and Robo3 were initially identified as axon guidance signaling molecules pairs in *Drosophila* and mice (Brose et al., 1999; Kidd et al., 1999; Blockus and Chedotal, 2016) that participate in wiring diverse regions of the nervous systems (Jen et al., 2004; Hao et al., 2001; Long et al., 2004; Spitzweck et al., 2010; Oliva et al., 2016). Upon Slit binding, Robo triggers an intracellular signaling cascade that leads to repulsion mediated by cytoskeletal remodeling in growth cones during axonal pathfinding (Blockus and Chedotal, 2016). However, recent work shows that this

* Corresponding author.
E-mail address: colivao@bio.puc.cl (C. Oliva).

https://doi.org/10.1016/j.ydbio.2019.10.004
Received 19 March 2019; Received in revised form 4 October 2019; Accepted 5 October 2019
Available online 10 October 2019

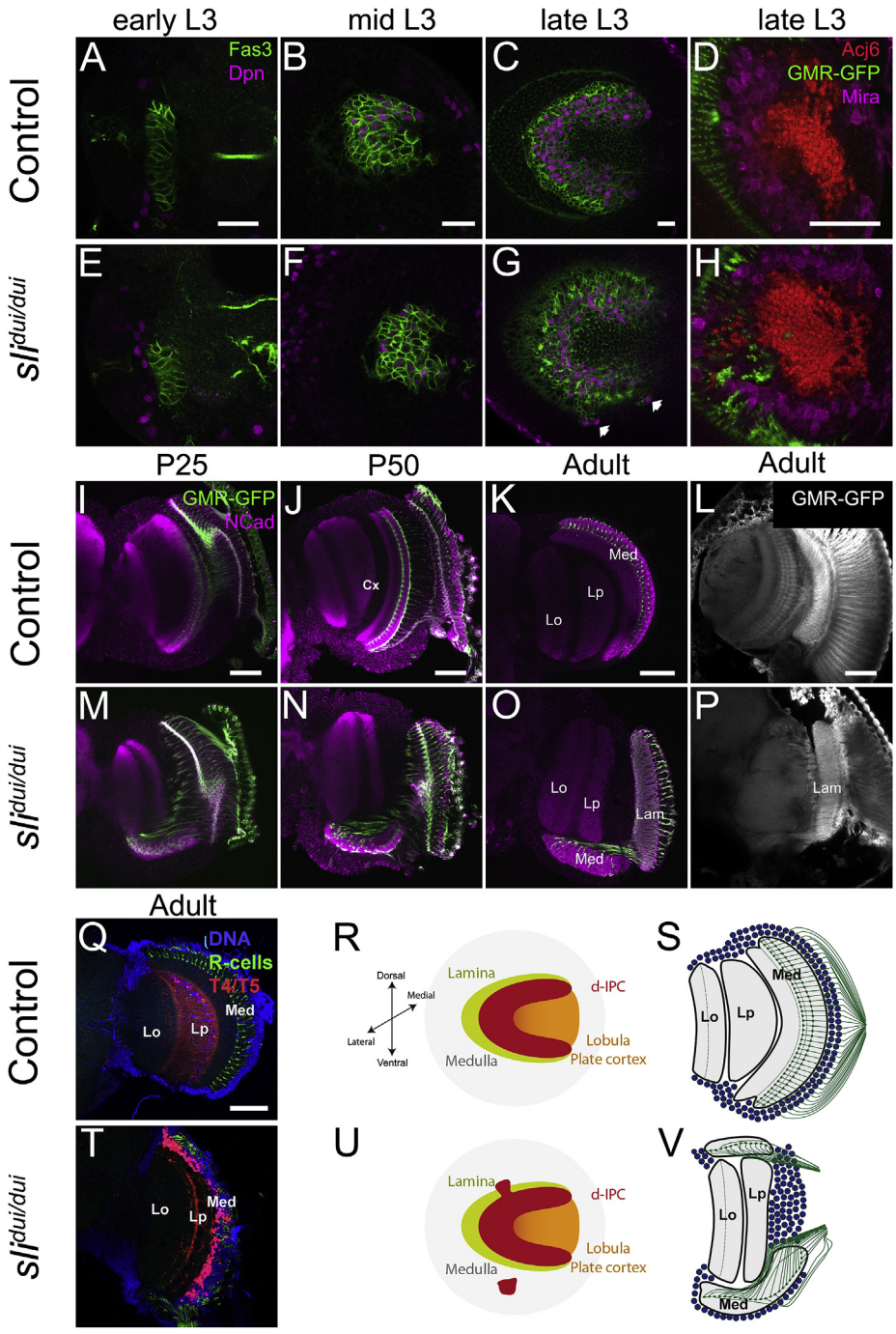

Fig. 1. Characterization of structural defects in *slit* mutants during development and in the adult optic lobe. Analysis of *slit* mutant defects in optic lobes during development and in adult animals. *GMR-GFP* labels R-cells; Fasciclin3 (Fas3, in green) marks IPC neuroblasts and their progeny (A-C, E-G); Deadpan (Dpn, in magenta) marks neuroblasts (A-C, E-G); Acj6 (in red) is a transcription factor expressed in lobula plate neurons (D and H); Miranda (Mira, in magenta, in D and H) labels neuroblast; N-Cadherin (NCad, in magenta) labels neuropils. (A–D) Control animals ($slit^{dui}$, *GMR-GFP*/CyO) and (E–H) $slit^{dui}$, *GMR-GFP* homozygous mutants in L3 stage (lateral section, anterior left). Note in (D) that IPC neuroblasts (Mira + cells) are segregated from the lamina precursor region (highlighted by R-cell axons in this view (GFP) and its progeny labeled with Acj6) in the wild type, but they intermingle in the mutants (H), arrowheads in (G) indicate ectopic neuroblasts. (I–L) Control animals ($slit^{dui}$, *GMR-GFP*/CyO) and (M–P) $slit^{dui}$, *GMR-GFP* homozygous mutants in pupal and adult samples (frontal section, medial left). Note that clear defects in optic lobe organization are observed (M–P). (Q) Control ($slit^{dui}$, *GMR-GFP*/CyO) and (T) *slit* homozygous mutant ($slit^{dui}$, *GMR-GFP*) adult optic lobes expressing *IPC-lexA* and *lexAop-mCherry* transgenes for visualization of T4/T5 neurons in adult samples (frontal sections, medial left). Note that in mutant animals T4/T5 cells are miss-localized to the presumptive medulla region. (R, S) Schemes representing L3 and adult organization in wild type and (U, V) in *slit* mutant animals. Scale bars represent 20 μm in (A–C), 25 μm in (D), 50 μm in (I-L, Q). Cx: Cortex, d-IPC: distal Inner Proliferation Center, Lam: Lamina, Lo: Lobula, Lp: Lobula plate, Med: Medulla.

pathway is also implicated in cell migration, boundary formation and cancer development, although the molecular targets are less clear (Blockus and Chedotal, 2016). After secretion, Slit is processed by an unknown protease to generate two fragments: N-Slit, which binds Robo, and C-Slit, which does not bind Robo, but participates in other signaling pathways (Brose et al., 1999; Coleman et al., 2010; Ordan et al., 2015). The relevance of this proteolytic processing is still not well established.

The *Drosophila* visual system is composed of the retina, which bears the photoreceptor cells (R-cells) that transduce the light stimulus, and four neuropils involved in the processing of the visual information. These neuropils are the Lamina, Medulla, Lobula and Lobula plate (Fig. S2A–B) (Ngo et al., 2017; Plazaola-Sasieta et al., 2017; Apitz and Salecker, 2014; Fischbach and Dittrich, 1989). During development, the outer proliferating center (OPC) gives rise to the lamina and the medulla, while the inner proliferating center (IPC) generates part of the medulla rim (the proximal region of the medulla (Neriec and Desplan, 2016)), the lobula and the lobula plate (Apitz and Salecker, 2014). Although many studies have addressed the molecular mechanisms underlying the specification of the different cell types of each neuropil, the formation of boundaries that ensure the integrity of these compartments is poorly understood. Previously, it was shown that the Slit/Robo pathway is implicated in this process (Tayler et al., 2004; Suzuki et al., 2016). In *slit* mutants and after knocking down all three Robo receptors in neurons, defects in boundaries between presumptive neuropils were reported at the larval stage. However, it is unclear in which cellular populations the expression of Slit protein and Robo receptors are required for the proper patterning and separation of the different compartments.

Here we carried out a systematic analysis of the contribution of Slit in

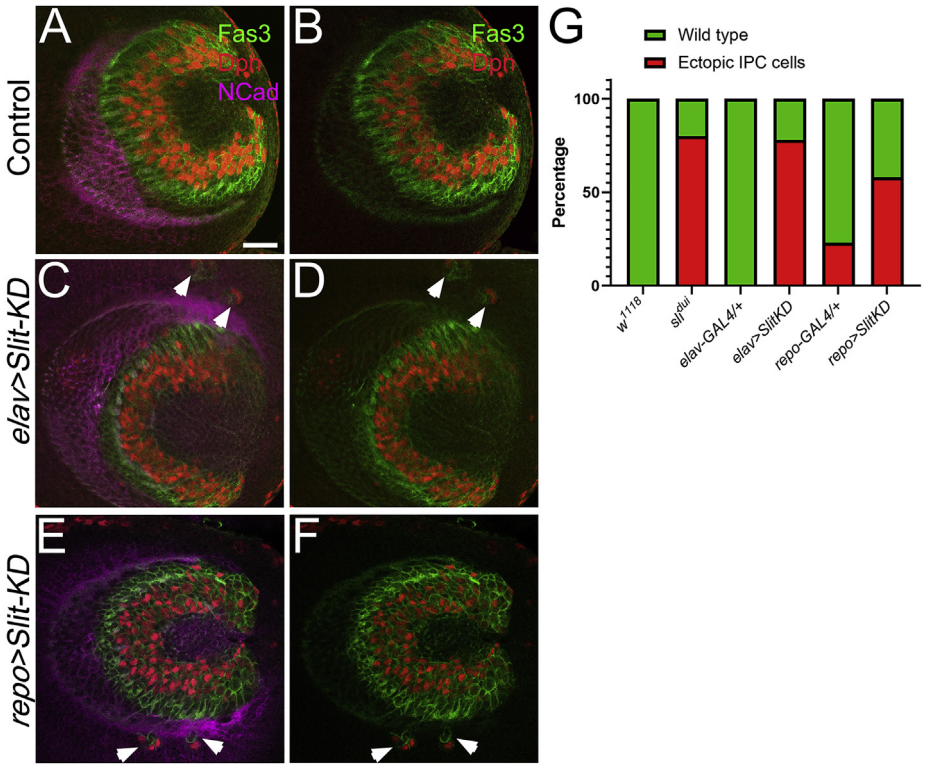

Fig. 2. ***slit*** **knockdown in neurons or glial cells leads to ectopic localization of IPC neuroblasts.** Lateral view of larval optic lobes immunostained against Fas3 (green), Dpn (red), and NCad (magenta), anterior is left. (A, B) Control brain. (C, D) *slit* knockdown in neurons using *elav-GAL4*. (E, F) *slit* knockdown in glial cells using *repo-GAL4*. Arrowheads highlight ectopic IPC neuroblasts in the medulla. (G) Quantification of the observed phenotypes. Scale bar represents 30 μm.

different cell populations for the proper formation of the visual system, using tissue specific knockdown and rescue of mutant phenotypes. We show that, unlike the previously accepted model in which glial cells are the main source of Slit, neuronal Slit is essential for the correct morphogenesis of the optic lobe. In this context, we determined that Slit function does not depend on cell-cell contact, as it has been reported in other systems (Ordan et al., 2015). Our results reveal that neuronal secretion of Slit is essential for optic lobe morphogenesis.

2. Results

2.1. Slit deficiency disrupts the organization of the adult optic lobe

The phenotypes generated by the loss of *slit* have been extensively described in larval stages (Tayler et al., 2004), however, the resulting defects in the pupal and adult neuropils are less known, and this characterization has been focused on the wiring of R-cells (Pappu et al., 2011; Plazaola-Sasieta et al., 2019). In order to describe these defects throughout development and in adult animals, we used different molecular markers and the previously characterized sli^{dui} mutant allele, a hypomorphic allele with reduced Slit expression especially in the visual system ((Tayler et al., 2004) and Fig. S1). First, we confirmed and extended the reported defects of this mutant in the lamina-lobula plate and medulla-lobula plate boundaries during larval development (Tayler et al., 2004; Suzuki et al., 2016). Thus, we found ectopic localization of IPC neuroblasts in *slit* mutant animals at late third instar stage, using the markers Deadpan (Dpn, (Wallace et al., 2000)) for neuroblast and Fasciclin3 (Fas3, (Apitz and Salecker, 2015)) for IPC cells (Fig. 1A–H). We also observed an aberrant intermingling between lobula plate neurons (Acj6+), IPC neuroblasts (Mira + cells) and R-cell axons in larval stage (Fig. 1D, H). Thus, our results indicate that Slit inhibits cell mixing between neuropils and prevents intermingling between IPC neuroblasts and their progeny that normally occupy distinct locations.

To highlight the architecture of the optic lobe in pupal and adult stages, we used the neuropil marker N-Cadherin (NCad) (Iwai et al., 1997) and a nuclear marker. Additionally, a *GMR-GFP* transgene in the sli^{dui} mutant background allowed us to follow the organization of R-cell axons. In pupal stages, the medulla was dramatically affected and the organization of R-cell axons was lost (Fig. 1I, J, M, N). In adult stage, the shape of the optic lobe appeared more elongated in frontal sections (Fig. 1K, L, O, P), a parameter that was quantified using the aspect-ratio (Fig. S2P), and clear architecture defects were observed in posterior confocal sections in all mutant samples. Remarkably, the typical layered organization of the medulla neuropil was lost. The lobula plate was clearly elongated in mutant animals compared to controls, while the organization of the lobula and lamina seemed more conserved (Fig. 1L, P). In horizontal sections, other aspects of the phenotypes can be observed (Fig. S2C–N). Thus, although the lamina seems less affected in *slit* mutants, its connections with the medulla through the outer optic chiasm were severely disrupted. Indeed, instead of connecting through the distal medulla, the lamina was connected to the medulla through its proximal region, next to the lobula plate (Fig. S2F and J and (Pappu et al., 2011)). Furthermore, analysis of horizontal sections using Fas3 antibody, which labels a subset of neuronal populations in the optic lobe, lobula plate T4/T5 and lamina neurons among them (Apitz and Salecker, 2015; Contreras et al., 2018; Mora et al., 2018; Oliva et al., 2014; Pinto-Teixeira et al., 2018; Apitz and Salecker, 2018; Contreras et al., 2019; Lin et al., 2016), showed ectopic projections in the medulla. Since T4/T5 neurons did not show ectopic projections in this region in the sli^{dui} mutant, this defects are likely to be originated from lamina neurons (See arrowheads in Fig. S2D and H). As observed in larvae, adult brains also displayed ectopic localization of IPC-derived cell populations such as lobula plate T4/T5 neurons misplaced in the proximal medulla (Fig. 1Q, T and Fig. S2K–N).

Finally, we assessed whether these defects have consequences in the perception of the visual stimulus. We used a standard phototaxis assay

Table 1
Summary of the phenotypes observed in the different experimental conditions.

Genotype	n (optic lobes)		
Knock-down experiments larval stage		Wild type	Ectopic IPC cells
w1118	9	100%	0%
$sli^{dui/dui}$,GMR-GFP	15	20%	80%
elav-GAL4/+	9	100%	0%
elav-GAL4/+; $sli^{Df(2R)BSC482}$/+; UAS-Slit-RNAi/+	9	22%	78%
repo-GAL4/+	13	77%	23%
$sli^{Df(2R)BSC482}$/+; repo-GAL4/UAS-Slit-RNAi	12	42%	58%

Genotype	n (animals)		% Neuropil defects		
Knock-down experiments adult animals		Wild type	Class I (Strong [a])	Class II (mild [a])	Class III (weak[a])
sli^{dui},GMR-GFP/CyO	27	100%	0%	0%	0%
$sli^{dui/dui}$,GMR-GFP	30	0%	100%	0%	0%
elav-GAL4/+	8	100%	0%	0%	0%
elav-GAL4/+; $sli^{Df(2R)BSC482}$/+; UAS-Slit-RNAi/+	12	0%	58%	42%	0%
repo-GAL4/+	17	100%	0%	0%	0%
$sli^{Df(2R)BSC482}$/+; repo-GAL4/UAS-Slit-RNAi	19	0%	5%	63%	32%
UAS-DCR2/+;; repo-GAL4, UAS-mCD8-GFP/+	25	100%	0%	0%	0%
UAS-DCR2/+; $sli^{Df(2R)BSC482}$/+; UAS-Slit-RNAi/repo-GAL4, UAS-mCD8-GFP	9	0%	0%	78%	22%
UAS-DCR2/+;UAS-mCD8-GFP/+;; ey^{OK107}-GAL4/+	8	100%	0%	0%	0%
UAS-DCR2/+;UAS-mCD8-GFP/$sli^{Df(2R)BSC482}$; UAS-Slit-RNAi/+; ey^{OK107}-GAL4	10	0%	80%	20%	0%
GMR-GAL4, UAS-mCD8-GFP/+	15	100%	0%	0%	0%
GMR-GAL4, UAS-mCD8-GFP/$sli^{Df(2R)BSC482}$; UAS-Slit-RNAi/+	9	0%	0%	44%	56%

Genotype	n (animals)		% Neuropil defects			
Rescue and ectopic expression experiments		Wild type	no rescue	Class I (weak)	Class II (mild rescue)	Class III (strong rescue)
sli^{dui},GMR-GFP/sli^{2}; UAS-Slit-HA/+	21	0%	100%	0%	0%	0%
L-GMR-GAL4/+	13	100%	0%	0%	0%	0%
sli^{dui},GMR-GFP/sli^{2}; L-GMR-Gal4/+	17	0%	100%	0%	0%	0%
sli^{dui},GMR-GFP/sli^{2}; L-GMR-GAL4/UAS-Slit-HA	15	0%	0%	0%	100%	0%
repo-GAL4/+	20	100%	0%	0%	0%	0%
sli^{dui},GMR-GFP/sli^{2}; repo-GAL4/+	21	0%	100%	0%	0%	0%
sli^{dui},GMR-GFP/sli^{2}; repo-GAL4/UAS-Slit-HA	16	0%	0%	75%	25%	0%
UAS-mCD8-GFP/+;;ey^{OK107}-Gal4/+	10	100%	0%	0%	0%	0%
sli^{2}/+; ;ey^{OK107}-GAL4/+	14	100%	0%	0%	0%	0%
sli^{dui},GMR-GFP/sli^{2};;ey^{OK107}-GAL4	26	0%	100%	0%	0%	0%
sli^{dui},GMR-GFP/sli^{2}; UAS-Slit-HA/+; ey^{OK107}-GAL4/+	20	70%	0%	0%	0%	30%
sli^{dui},GMR-GFP/sli^{2}; UAS-Slit-TM-myc/+; ey^{OK107}-GAL4/+	15	0%	100%	0%	0%	0%
sli^{dui},GMR-GFP/sli^{2}; UAS-Slit-UC-myc/+; ey^{OK107}-GAL4/+	13	0%	0%	0%	0%	100%
UAS-Slit-HA/+; ey^{OK107}-GAL4/+	10	100%	0%	0%	0%	0%
UAS-Slit-TM-myc/+; ey^{OK107}-GAL4/+	10	100%	0%	0%	0%	0%

[a] The phenotypes of the same category may not be equal across genotypes.

(Gorostiza et al., 2016) and found that *slit* mutants did not respond to the light as control animals did (Fig. S2O). Hence, *slit* mutants display several morphological defects in the optic lobe and physiological deficiencies as consequence of aberrant boundary formation, cell migration and axon guidance defects during development (Fig. 1R, S, U, V).

2.2. Slit is mainly required in neurons during optic lobe development

Previous reports have assumed that Slit is mainly secreted by the glial cells in the lamina-medulla and lamina-lobula plate boundaries (Tayler et al., 2004; Pappu et al., 2011; Fan et al., 2005; Chotard and Salecker, 2007; Edwards et al., 2012) even though Slit is also expressed by neurons of the medulla ganglion (Tayler et al., 2004; Pappu et al., 2011). No definitive functional studies have been performed to demonstrate the relevance of these Slit sources. In order to clarify this issue, we knocked down *slit* expression, using a previously validated RNAi line (Oliva et al., 2016; Suzuki et al., 2016, 2018; Biteau and Jasper, 2014), in neurons or glial cells using *elav-GAL4* or *repo-GAL4* drivers respectively (Fig. 2A–F). In larval brains, *slit* knockdown with both drivers produced ectopic IPC cell clusters outside their normal region, similar to what was observed in *slit* mutant animals. Interestingly, the penetrance of this phenotype was higher when *slit* was knocked down in neurons (Fig. 2G and Table 1). This was not due to higher levels of expression of the *elav-GAL4* compared to *repo-GAL4* driver (Fig. S3).

Next, we examined the effect of *slit* knockdown on the adult visual system (Fig. 3A–O and Table 1). We observed defects in the adult optic lobe organization upon *slit* downregulation in glial cells, however, the general morphology of the optic lobe was less affected than in *slit* mutants (compare Fig. 3G–I to D–F). The ratio between the distal medulla cortex and optic lobe areas decreased upon *slit* knockdown (control: $0.1016 \pm 0{,}01034$, $n = 17$ and Repo > SlitKD: $0{,}05222 \pm 0{,}01687$, $n = 19$, $p < 0{,}0001$), suggesting that fewer cells were present in this region. On the other hand, the aspect-ratio was similar to control animals (Fig. 3M). Surprisingly, knocking down *slit* in neurons led to strong phenotypes (Fig. 3J–L, O). The morphology of the optic lobe appeared elongated, comparable to *slit* mutant animals, while the organization of the cell bodies also resembled the mutant phenotype (Fig. 3J–L), and the aspect-ratio was higher than controls (Fig. 3N). Therefore, these experiments indicate that the neuronal source of Slit explains most of the defects observed in *slit* mutants.

2.3. Slit expression in medulla neurons is required for the development of the Drosophila visual system

Next, we explored the expression of Slit in different neuronal populations of the visual system. Adult medulla neurons can be covered almost completely using the expression of three enhancer-trap lines in the promoter regions of the transcription factors encoded by the genes *eyeless* (*ey*), *apterous* (*ap*) and *distal-less* (*dll*) (Morante and Desplan, 2008) (Fig. S4A–C). Importantly, these transcription factors are expressed in

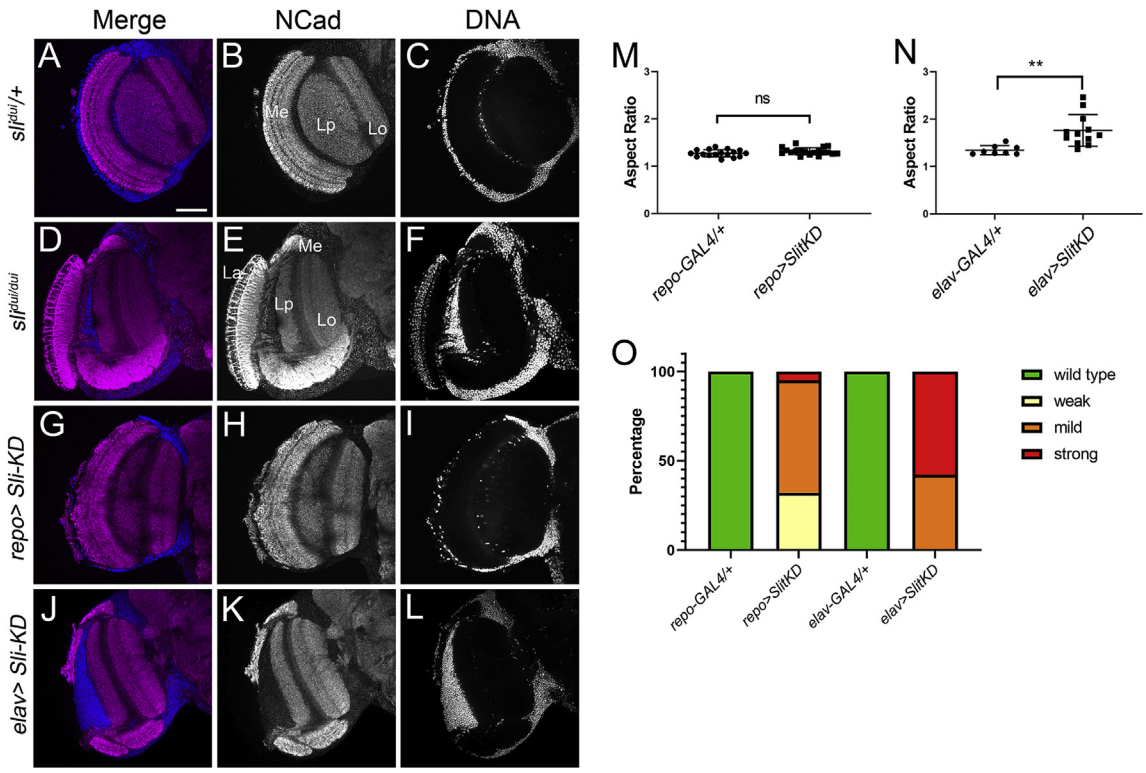

Fig. 3. Slit is required in neurons for optic lobe morphogenesis. (A–L) Adult brains immunostained against NCad (neuropile, in magenta or gray) and counterstained with Hoechst (DNA, in blue or gray). (A–C) Optic lobes of $slit^{dui/+}$ heterozygous animals. (D–F) $slit^{dui}$ mutant animals. (G–I) *slit* knockdown in glial cells using *repo-GAL4*. (J–L) *slit* knockdown in neurons using *elav-GAL4*. Note that knocking down *slit* in neurons causes similar defects than mutant animals, while decreasing *slit* in glia has weak defects. (M–N) Quantification of the aspect-ratio in the different conditions (** = $p < 0.01$, ns: non-significant, Two-tailed Student's t-test). (O) Quantification of the frequency of observed phenotypes in each condition. Scale bar represents 50 μm. La: Lamina, Lo: Lobula, Lp: Lobula plate, Me: Medulla.

non-overlapping populations of medulla neurons. We tested these lines in the larval brain and found that ap^{md544}-*GAL4* and ey^{OK107}-*GAL4* drivers were expressed specifically in broad subsets of developing medulla neurons (Fig. S4D–E), as previously reported (Morante et al., 2011). Meanwhile, dll^{md23}-*GAL4* was expressed in very few cells and none of them established projections in the Slit enriched area of the medulla neuropil at this stage. Instead, a group of cells residing in the lamina, which was also covered by dll^{md23}-*GAL4*, sent projections to the Slit enriched region (Fig. S4F). Interestingly, careful examination of Ey + neurites showed that they co-localized largely with Slit staining (Fig. 4A–B). To complement our expression analysis we used an endogenous Slit-GFP fusion protein (Venken et al., 2011) that underlines cell membranes (Plazaola-Sasieta et al., 2019). This construct showed expression in Ey + neurons (Fig. 4C–D) indicating that indeed Ey + neurons express Slit. Ey + medulla neurons sent projections adjacent to the boundary between lamina and medulla where the lamina glia is positioned (Fig. 4E–F). Furthermore, we found that Slit is also present in R-cells in the L3 eye imaginal disc using the anti-Slit antibody (Fig. 4G–H) and the Slit-GFP line (Fig. S5), indicating that Slit is secreted by different neuronal populations.

Based on these results we asked whether there is a requirement for Slit expression in specific neuronal populations of the visual system. Because we observed that cell bodies expressing the *ey* and *ap* drivers were localized in the medulla starting at the L3 stage, we used ey^{OK107}-*GAL4* and ap^{md544}-*GAL4* to knockdown *slit* in each of these neuronal populations. We observed optic lobe defects upon *slit* knockdown in these two populations (Fig. S6A–P); however, the knockdown in Ey + neurons elicited the strongest phenotypes, resembling those of the *slit* mutant. Furthermore, *slit* knockdown in Ey + neurons led to ectopic localization of IPC cells in L3 stage (Fig. S7), supporting a role of Slit from medulla neurons for proper boundary formation in the optic lobe.

Next, we compared the effect of knocking down the expression of *slit* in Ey + medulla neurons to the effect in glial cells and R-cells (Fig. 5A–X and Table 1). We found that *slit* downregulation in R-cells, using the *GMR-GAL4* driver, led to loss of regions in the medulla, but this phenotype was mild. On the other hand, R-cell innervation of the medulla was disrupted. Glial knockdown of *slit* also disturbed the innervation pattern of R-cells in the optic lobe besides the medulla defects (Fig. 5P). Finally, quantification of the aspect-ratio showed that only knockdown in Ey + medulla neurons led to elongated optic lobes resembling the *slit* mutant phenotype. All together, these data suggest that Slit is required in Ey + neurons for the correct boundary formation and morphogenesis of the optic lobe, although the expression in the eye primordium and glial cells also contribute to this process.

2.4. Re-expression of slit in Ey + medulla neurons restores optic lobe morphology in the slit mutant background

Previous experiments using widely expressed optic lobe drivers have suggested that Slit reintroduction can rescue larval defects (Tayler et al., 2004). Since knockdown experiments indicated that Slit is required in medulla neurons, we wondered whether reintroduction of Slit in a cell-type specific fashion (i.e. in glial cells, Ey + medulla neurons, and in R-cells) could rescue the optic lobe defects seen in *slit* mutants (Fig. 6A–X and Table 1). For these experiments, we used the allelic combination of $slit^{dui}$ with the null $slit^{2}$ allele that generate a non-functional truncated protein (Bhat et al., 2007), whose phenotype is milder than the one observed in $slit^{dui/dui}$ animals. Although we found partial improvements in some aspects of the mutant phenotypes when Slit was reintroduced in glia or R-cells (Fig. 6I–P, V, X and Table 1), the expression of Slit in medulla neurons using ey^{OK107}-*GAL4* driver led to an almost full rescue of the adult optic lobe morphology (Fig. 6Q–T, W, X and Table 1). Thus, our

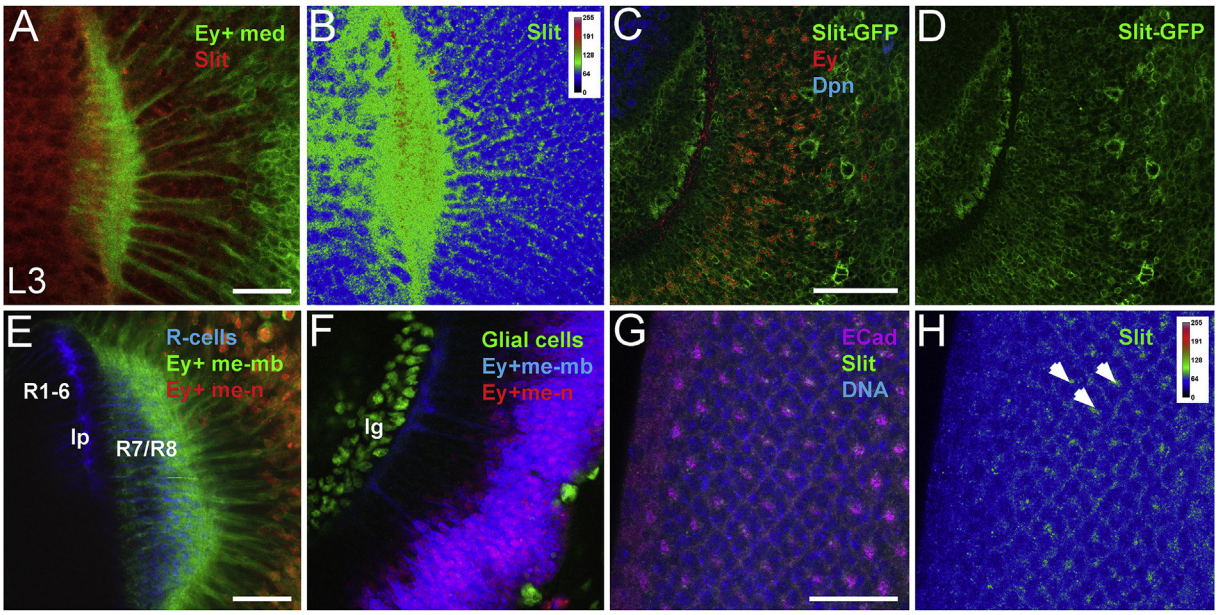

Fig. 4. Slit protein is expressed in Ey + medulla neuron projections. (A) Larval optic lobe of animals expressing mCD8-GFP under the control ey^{OK107}-GAL4 immunostained with anti-Slit antibody. (B) Color-coded image of Slit levels, pixel intensity scale is indicated. (C, D) Larval optic lobes of animals expressing Slit-GFP MIMIC-RMCE construct, in this construct Slit is only observed in cell membrane. Immunostaining of Eyeless transcription factor (red) and Dpn (blue) allow visualization of Ey + medulla neurons and neuroblasts respectively. Note that a subset of cells expressing Slit-GFP are positive for Ey. (E) Optic lobe of L3 brain expressing a mCD8-GFP reporter for the Ey + medulla neurons membrane and mCherryNLS (NLS: nuclear localization sequence) for the nuclei. R-cell axons are labeled in blue using 24B10 antibody. Note the close proximity between medulla neurites and retinal axons. (F) Optic lobe of L3 brain expressing medulla Ey + neuron reporters (membrane: blue, nuclei: red) and immunostained with the glial marker Repo (green). Lamina glial cells are located next to medulla neurites (blue). (G) L3 eye disc stained for E-cadherin (ECad, magenta), Slit (green) and Hoechst (DNA, blue). (H) Color-coded image of Slit expression, pixel intensity scale is indicated. Ey + med: Eyeless positive medulla neurons, Ey + me-mb: Ey + medulla neuron membrane, Ey + me-n: Ey + medulla neuron nuclei, lg: Lamina glia, lp: lamina plexus. Scale bars represent 20 μm in (A), 50 μm in (C) and 20 μm in (E) and (G).

data strongly suggest that Slit expression in medulla neurons is necessary for optic lobe development and re-expression in Ey + neurons can rescue the normal optic lobe architecture in *slit* mutant animals.

2.5. *Slit secretion but not proteolytic processing is required for optic lobe development*

Slit is a secreted protein that has been proposed to form a gradient providing axons with positional information during their navigation, in the developing nervous system. However, in some contexts Slit seems to work in a manner that requires cell-cell contact (Kraut and Zinn, 2004). We asked whether a form of Slit that is tethered to the cell membrane can still rescue the *slit* mutant phenotype when expressed in Ey + medulla neurons (Fig. 7A–P, U–V and Table 1). In order to do this, we directed the expression of a version of N-Slit (which is the processed form and is known to bind to Robo receptors) harboring a CD8 transmembrane domain (N-Slit-TM) to this cell population. Upon expression of N-Slit-TM, the phenotypes observed were indistinguishable from those of the *slit* mutants (Fig. 7E–H, M–P, U–V and Table 1), indicating that, in this context, Slit has to be secreted into the extracellular. Importantly, ectopic expression of this construct in a wild type background did not have a dominant effect (Fig. S8 and Table 1) and it was detected in Ey + neurons upon expression (Fig. S9A and F).

After secretion, Slit is processed to give rise to an N-terminal fragment that binds Robo receptors and a C-terminal region, recently implicated in the Sema/Plexin signaling in vertebrates (Delloye-Bourgeois et al., 2015). It has previously been shown that this processing is essential during *Drosophila* muscle development, in which an uncleavable form of Slit (Slit-UC) knocked into the *slit* locus present defects in this system (Ordan et al., 2015). However, the expression of Slit-UC in a *slit* mutant background rescues embryo VNC defects as efficiently as the wild type form during commissure formation (Coleman et al., 2010), indicating a differential requirement for this processing in a context dependent manner. We decided to test whether the Slit-UC could rescue the optic lobe defects upon expression in Ey + medulla neurons (Fig. S9E and F; Fig. 7Q–T, U–V and Table 1). We observed a strong rescue similar to that obtained using the wild type form of Slit, indicating that the processing of Slit is not required in this context, although Slit has to be secreted in order to work properly.

3. Discussion

Here we used mutant alleles, RNAi-mediated knockdown, and cell specific rescue experiments to show that Slit, provided by medulla neurons, regulates the establishment of the neuropil boundaries and morphogenesis of the optic lobe (Fig. 8). Furthermore, we demonstrate that Slit has to be secreted by medulla neurons in order to control neuropil organization, whereas the proteolytic processing of Slit is not required for its function as it is observed in other contexts.

3.1. *Axon guidance and boundary formation during optic lobe morphogenesis*

In the developing optic lobe, we can distinguish the regions that will form each neuropil in the adult. It has been reported that boundaries expressing Slit constrain cells and certain axons in each compartment, avoiding cell mixing between the lobula complex and lamina (Tayler et al., 2004), and between lobula complex and medulla (Suzuki et al., 2016). Our results show that this is also true for cell populations (neurons and neuroblasts) within the IPC compartment. Interestingly, since Slit is required for axon guidance and cell positioning, these two processes need to be coordinated in order to achieve the final pattern. It is possible that Slit constrains cell migration in a similar manner to axon guidance, since it is well established that both processes share common molecular

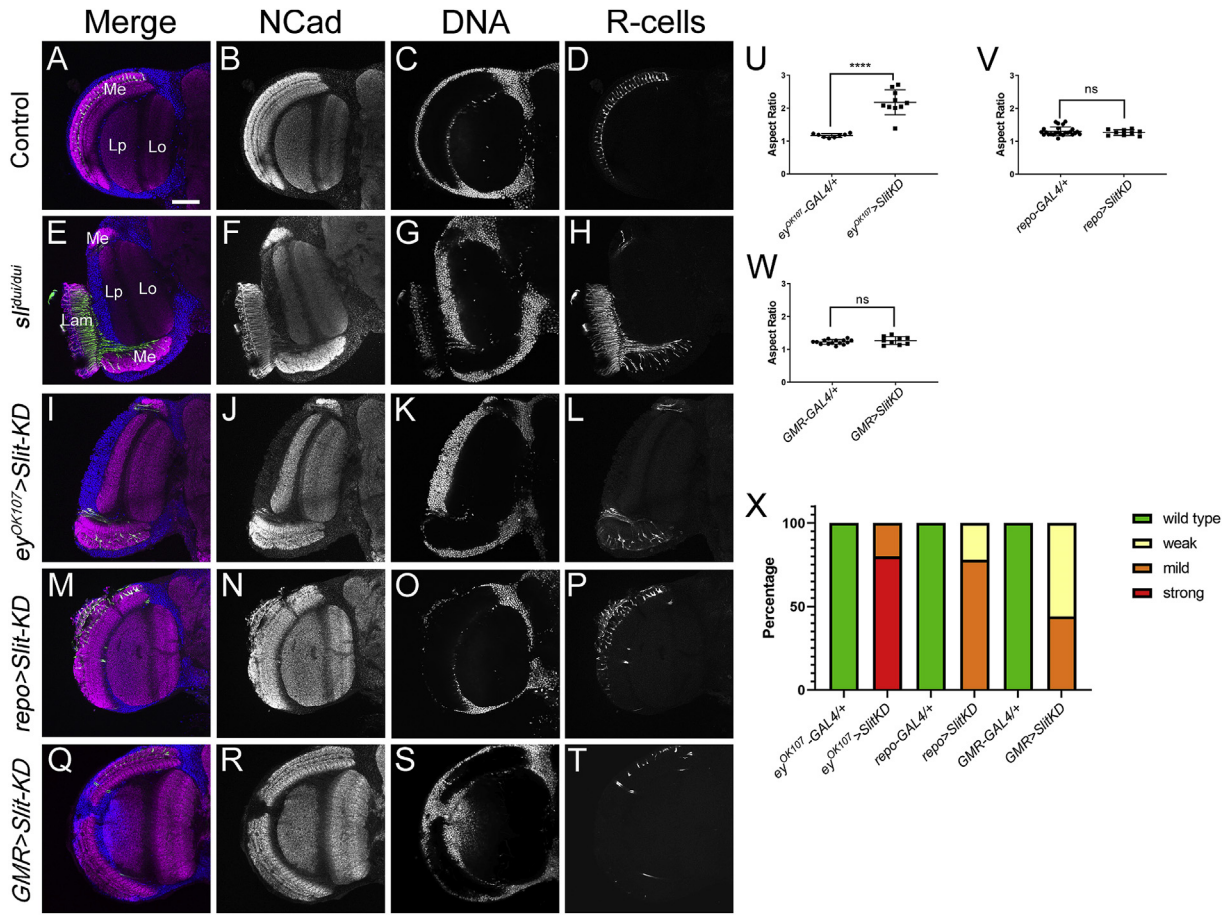

Fig. 5. Slit is required in Ey + medulla neurons for optic lobe development. Adult brains were immunostained with anti-NCad (neuropils, in magenta or gray), Hoechst (DNA, in blue or gray) and 24B10 antibody (retinal axons, in green or gray). (A–D) Control and (E–H) $slit^{dui/dui}$ mutant optic lobes. Note the dramatic change in optic lobe morphology of mutant compared to control animals. (I–L) Similar defects to the mutant are observed upon RNAi knockdown of *slit* expression in Ey + medulla neurons using ey^{OK107}*-GAL4* driver. (M–P) Knocking down *slit* expression in glial cells using the *repo-GAL4* driver results in disorganization of the retinal axons, but without dramatically affecting the general morphology of the optic lobe. (Q–T) *slit* knockdown in R-cells, using *GMR-GAL4* driver, causes sporadic gaps in the medulla neuropil. Lam: Lamina, Me: Medulla, Lp: Lobula plate, Lo: Lobula. (U–W) Quantification of the aspect-ratio in the different conditions (**** = $p < 0.0001$, Two-tailed Student's t-test). (X) Quantification of the frequency of the observed phenotypes in each condition, categories refer to the severity of the phenotype and images shown are representative of the most frequent category. Scale bar represent 50 μm.

mechanisms (Branda and Stern, 1999; Brose and Tessier-Lavigne, 2000; Tsai and Miller, 2002). It will be interesting to test this hypothesis in the context of optic lobe development. Although much is known about the molecules that regulate axon guidance, such as Netrin/Frazzled, Semaphorins and Slit/Robo, less has been studied about the mechanisms behind boundary formation and how these pathways crosstalk with axon guidance pathways. However, it is clear that boundaries are also choice points for axon sorting; for instance the lamina/medulla border also serves to sort R1-R6 axons, which stay in the lamina, from R7-R8, which reside in the medulla (Ngo et al., 2017).

3.2. Secreted cues govern neuropil boundary formation

Research on boundary formation in multiple systems has identified three basic mechanisms: differential cell adhesion, cortical tension and cell-cell contact mediated repulsion by Ephrin and Ephrin receptors (also involved in axon guidance) (Batlle and Wilkinson, 2012). We further characterized the contribution of Slit, a secreted cue, to this process. Two previous articles have reported the function of Slit during boundary formation in the optic lobe (Tayler et al., 2004; Suzuki et al., 2016). However, given the complex expression pattern of Slit in this system, the participation of specific cell populations was still unclear. Our work provides evidence to support Slit secretion by multiple cell populations in the optic lobe, although medulla neurons seem to be the major contributor for the proper establishment of neuropil boundaries (Fig. 8).

In some contexts, secreted cues such as Netrin work in cell-cell interactions (Timofeev et al., 2012; Akin and Zipursky, 2016; Brankatschk and Dickson, 2006). Here, we studied what form of Slit is required for optic lobe formation and boundary establishment. Our results indicate that Slit needs to be secreted to work properly. In light of these findings, Slit, like other secreted molecules such Netrin, are starting to be considered in the process of boundary formation (Suzuki et al., 2018).

How might this secreted molecule regulate boundary formation? A new view is emerging from multiple systems showing that Slit is a component of the extracellular matrix (ECM) (Bhat, 2017). Thus, a possibility is that ECM-bound Slit can act as a restrictive barrier for growth cones or cells expressing Robo receptors on their surface. It would be interesting to test the participation of ECM components in boundary formation in future research.

3.3. Requirement of slit processing in nervous system development

Slit processing was described long ago (Brose et al., 1999), but the requirement for its cleavage has remained obscure until recently. This is an interesting point since N-Slit can bind and activate Robo receptors at least in cell culture (Chen et al., 2001). In *Drosophila*, two reports have

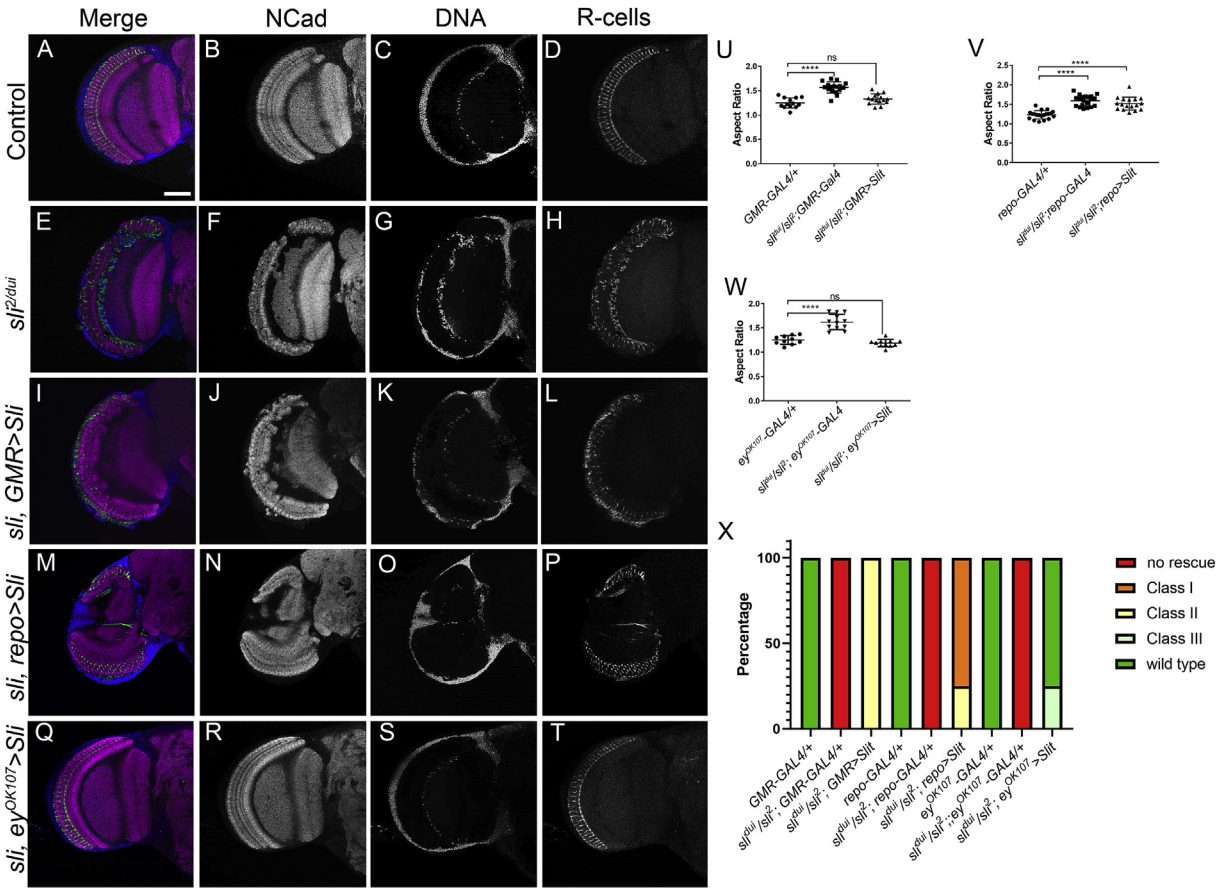

Fig. 6. Slit re-expression in medulla neurons rescues the mutant phenotype in the optic lobe. Adult brains were immunostained with anti-NCad (neuropils, in magenta or gray), Hoechst (DNA, blue or gray) and 24B10 antibody (R-cell axons, in green or gray). (A–D) Optic lobe of control animals. (E–H) $sli^{2/dui}$ mutant. (I–L) Slit re-expression in R-cells using *GMR-GAL4* driver. (M–P) Rescue experiment in glia using *repo-GAL4* driver. (Q–T) Slit rescue in medulla neurons using ey^{OK107}*-GAL4* driver. Note that reintroduction of Slit only in medulla neurons restores completely the wild type phenotype. (U–W) Quantification of the aspect-ratio in the different conditions (**** = $p < 0.0001$, one-way ANOVA). (X) Quantification of the frequency of the observed phenotypes in each condition, images shown are representative of the most frequent category. Categories are class I: weak rescue, class II: mild rescue, class III: strong rescue. Scale bar represents 50 μm.

analyzed this process *in vivo*. The work by Ordan et al. (2015) found that Slit cleavage is needed to allow the association of the N-Slit fragment with tendon cells and guide the migration of muscle progenitors. On the other hand, in the ventral nerve cord Slit proteolytic processing is not required for its function (Coleman et al., 2010). In the optic lobe, we found that Slit processing is dispensable, indicating that the cleavage requirement is highly context specific. In vertebrates, the C-Slit fragment can bind to another guidance receptor, PlexinA1 (Delloye-Bourgeois et al., 2015). However, it has not been established whether this is a common signaling mechanism for the C-Slit fragment.

3.4. Towards a model for the understanding function during the development of the fly optic lobe

Recently, Suzuki et al. proposed a mathematical model in which differential expression of Netrin, Slit, and their receptors in neurons and glia, is sufficient to explain the segregation between developing neuropils in the larval optic lobe (Suzuki et al., 2018). Nevertheless, this model does not take into account the secretion of Slit from medulla neurons. We propose that Slit secreted by medulla neurons act together with glial Slit to establish the lamina-lobula plate, and medulla-lobula boundaries. It will be interesting to test Suzuki et al. mathematical model in the light of our new data.

Our findings support a model in which Slit is secreted by different cell populations to form the boundaries between neuropils of the optic lobe (Fig. 8), but with differential contributions. Thus, loss of Slit in a cell-type specific manner leads to defects in optic lobe architecture, although with distinct severities. In every situation, there are defects in medulla architecture but the dramatic defects of *slit* mutants are phenocopied only after knockdown in Ey + medulla neurons. Interestingly, although knockdown of *slit* in glial cells and neurons lead to similar defects in larval stage (although with different penetrance), the impact of neuronal loss of Slit in the adult architecture is much stronger. This support the idea that Slit secreted by neurons, contributes with additional functions beyond boundary formation in this system. In summary, our results provide a novel view in which medulla neurons actively participate in the compartmentalization of the fly optic lobe and its wiring by the secretion of Slit.

4. Materials and methods

4.1. Fly husbandry

Flies were kept at 25 °C or 29 °C (for RNAi experiments) on standard medium. The lines used in our study were obtained or generated using flies strain from the Bloomington *Drosophila* Stock Center (Bloomington, Indiana). Other strains have been described previously by us (Contreras et al., 2018) or generated during this study. Detailed description of the genotypes can be found in Table S1.

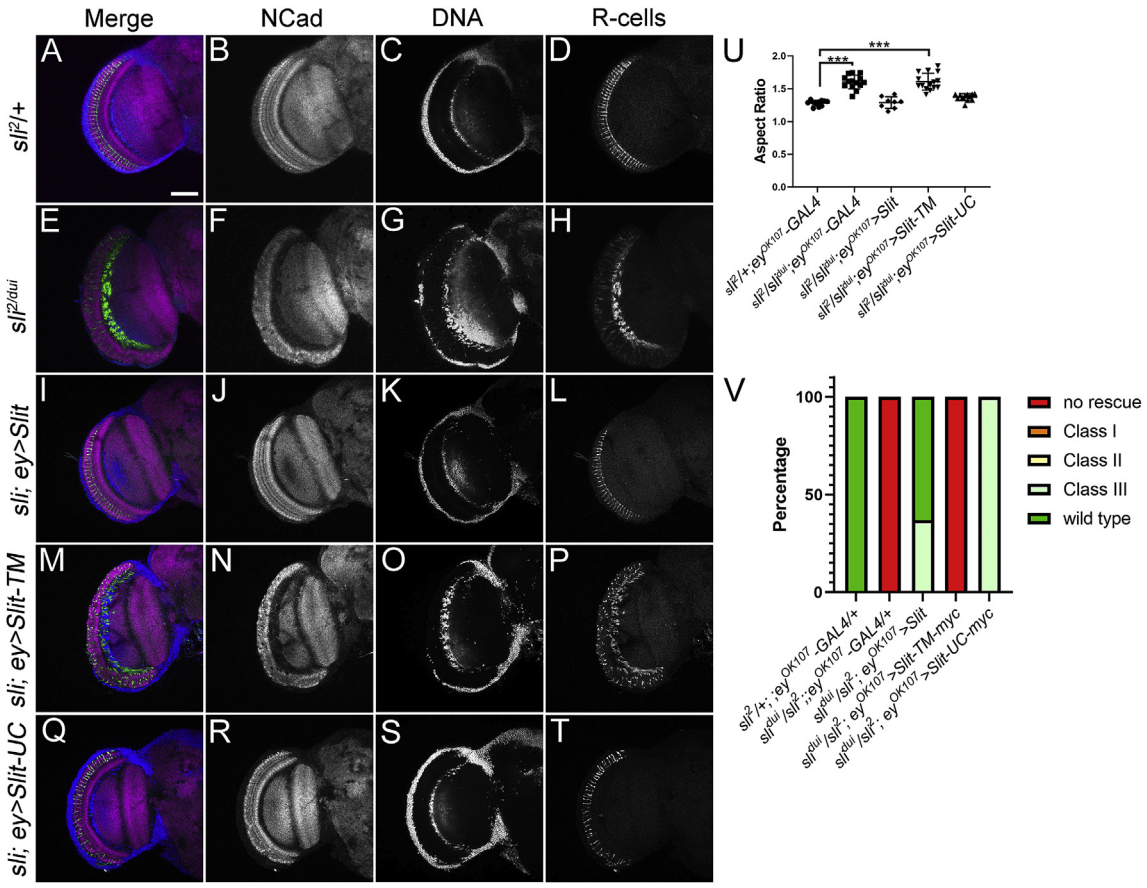

Fig. 7. Slit secretion is required for the correct development of the optic lobe. Adult brains were stained against NCad (neuropils, in magenta or gray), Hoechst (DNA, in blue or gray) and 24B10 antibody (R-cell axons, in green or gray) (A–D) *sli*^{2}/+ heterozygotes shows a wild type phenotype. (E–H) *sli*$^{2/dui}$ mutant animals. (I–L) Rescue expressing wild type Slit in medulla neurons using *ey*^{OK107}*-GAL4*. (M–P) Introduction of a membrane-tethered version of Slit (N-Slit-TM) does not rescue the mutant phenotype. (Q–T) Introduction of an uncleavable version of Slit (Slit-UC) is almost as effective as wild type Slit in rescuing the mutant phenotype. (U) Quantification of the aspect-ratio comparing the different conditions (**** = $p < 0.0001$, one-way ANOVA). (V) Quantification of the frequency of the observed phenotypes in each condition, images shown are representative of the most frequent category. Categories are class I: weak rescue, class II: mild rescue, class III: strong rescue. Scale bar represents 50 μm.

4.2. Generation of slit constructs

Slit UC construct was designed removing 39 nucleotides corresponding to a sequence between the 5th and 6th EGF domains containing the cleavage site (HNMISMMYPQTSP) as previously performed (Ordan et al., 2015). A Myc tag was also added to the C-terminus using a linker peptide (IASKPKGASVRA).

The Slit-N-CD8 construct was created by deleting the C-terminal fragment (the peptide indicated above plus the rest of the C-Terminus) and adding a CD8 sequence linked to the rest of the protein by the same linker peptide, followed by a Myc tag, also with this linker peptide.

These constructs were synthesized by Genewiz and cloned into the pUAST-attB vector. Transgenic flies were generated by Bestgene, Inc., USA.

4.3. Staining

Adult, pupal and third instar larval brains and eye discs were dissected and stained using standard procedures (Contreras et al., 2018; Walther and Pichaud, 2006; Wu and Luo, 2006). For vibratome sections, adult heads were detached from the body, and proboscis and antennae were removed. Heads were fixed in 8% formaldehyde in 1x PBS at 4 °C overnight. Heads were washed 3 times in 1x PBS. The samples were embedded in 8% Agarose in H_2O and 50–100 μm sections were obtained using a Leica VT1000S vibratome.

The following monoclonal antibodies were obtained from Developmental Studies Hybridoma Bank: rat anti-N-Cadherin (DN-Ex #8; 1:20) rat anti-DE-Cadherin (DCAD2; 1:20), mouse anti-Slit (C555.6D; 1:50), mouse anti-Acj6 (1:10), mouse anti-Chaoptin (24B10; 1:20), mouse anti-Fasciclin3 (7G10; 1:20), mouse-anti-Eyeless (1:10). Other antibodies used were guinea pig anti-Dpn (1:5,000, kind gift from Dr. Andrea Brand), rabbit anti-Miranda (1:500, kind gift from Dr. Yuh-Nung Jan), mouse anti-Myc (1:100; sc-40, Santa Cruz Biotechnology) and rabbit anti-GFP (1:1000; Invitrogen A11122). Fluorescent-dye conjugated secondary antibodies were obtained from Jackson Immunoresearch and used 1:200. Hoechst was used as DNA counterstain (1:1000).

4.4. Light/darkness assay

Light/darkness choice was measured in a T-maze as previously reported (Gorostiza et al., 2016). Briefly, a standard *Drosophila* T-maze was wrapped with aluminum foil to get only one transparent choice tube (bright tube). 24 h before experiments, 30 male flies (3–6 days old) were anesthetized with CO_2 and placed on normal food. The day of the experiment flies were transferred to the entrance tube in the T-maze and left in darkness for 10 min (adaptation time). They were then transferred to the cylindrical elevator chamber by gently tapping the apparatus. Afterwards, the flies are allowed to choose between the dark and the bright tubes, for 30 s. The light source, a fluorescent lamp, was placed 31.5 cm away from the bright choice tube of the T-maze. To avoid any

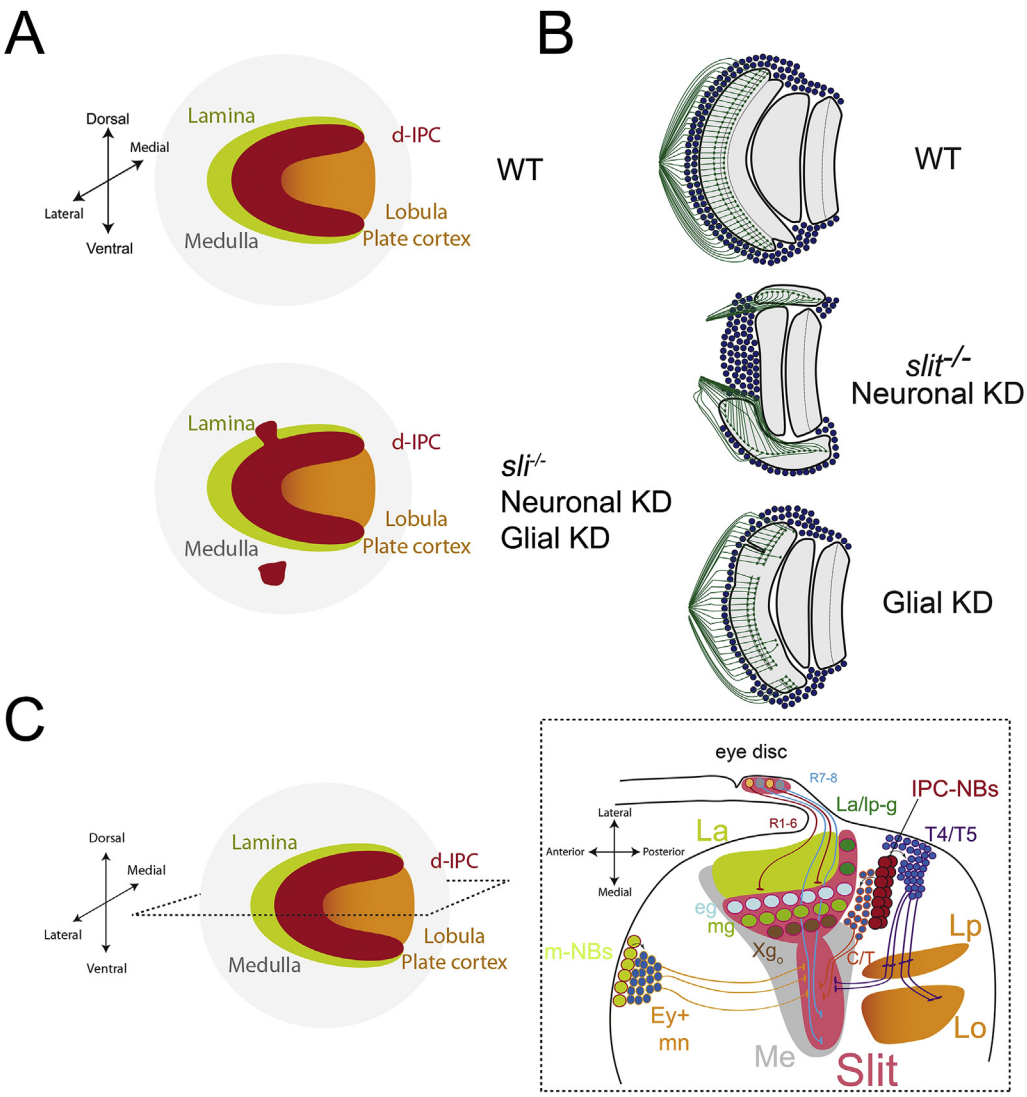

Fig. 8. Result summary and model of Slit function in optic lobe development. Schematic representations of normal and defective patterns in the late third instar larval stage (A) and adult (B) optic lobes. (C) Model of Slit function in optic lobe morphogenesis, horizontal section of the L3 system is depicted in the right. Some of the main cell populations in the optic lobe are indicated. Regions expressing Slit labeled in pink. R1-6 and R7-8 represent outer and inner R-cells, respectively, La: lamina, eg: epithelial glia, mg: marginal glia (eg and mg form the lamina glia), Xg_o: outer chiasm glia, la/lp-g: lamina-lobula plate border glia, IPC-NBs: inner proliferation center neurblasts, m-NBs: medulla neuroblasts, Ey + mn: Eyeless expressing neurons, C/T: neurons of the lobula plate, T4/T5: neurons of de lobula plate. Lp: lobula plate, Lo: lobula, Me: medulla.

choice bias, half the experiments were performed with the light source at the left side of T-maze and half at the right side. Experiments were carried out at 25 °C and 60% humidity.

4.5. Imaging

Images were obtained using an Olympus Fluoview-Fv1000, Zeiss 700 and Nikon confocal microscopes. All images were processed with Image J software (NIH) and the montage of figures performed with Adobe Photoshop CC. Schemes were designed using Adobe Illustrator CS3.

4.6. Data analysis and quantifications

Aspect-ratio was obtained using Image J software, for this purpose the perimeter of the optic lobe (without considering the lamina and retina) was drawn using a computer with a touch-screen monitor. Data analysis was performed with Graphpad Prism software. Two-tailed Student's *t*-test was used for two group comparisons and one-way ANOVA for multiple groups (Dunnett's multiple comparison test). Data were presented as mean ± standard deviation.

Acknowledgements

We are grateful to the Advanced Microscopy Facility UC for support in image acquisition, the Hybridoma Bank for antibodies and the Bloomington stock Center for fly strains. We thank Estela Andrés y Katia Gysling for providing equipment and members of the Oliva and Campusano lab for discussions. We would like to thank John Ewer for critically revising the manuscript.

Appendix A. Supplementary data

Supplementary data to this article can be found online at https://doi.org/10.1016/j.ydbio.2019.10.004.

Funding

This work was supported by CONICYT FONDECYT Initiation on Research # 11150610, CONICYT FONDECYT Regular #1191424 and ECOS-CONICYT 170009 to C.O., VIB to B.A.H. and CONICYT FONDECYT regular #1171800 and ICM P09-015-F to J.S.

References

Akin, O., Zipursky, S.L., 2016. Frazzled promotes growth cone attachment at the source of a Netrin gradient in the Drosophila visual system. Elife 5.
Apitz, H., Salecker, I., 2014. A challenge of numbers and diversity: neurogenesis in the Drosophila optic lobe. J. Neurogenet. 28, 233–249.
Apitz, H., Salecker, I., 2015. A region-specific neurogenesis mode requires migratory progenitors in the Drosophila visual system. Nat. Neurosci. 18, 46–55.

Apitz, H., Salecker, I., 2018. Spatio-temporal relays control layer identity of direction-selective neuron subtypes in Drosophila. Nat. Commun. 9, 2295.
Batlle, E., Wilkinson, D.G., 2012. Molecular mechanisms of cell segregation and boundary formation in development and tumorigenesis. Cold Spring Harb. Perspect. Biol. 4, a008227.
Bhat, K.M., 2017. Post-guidance signaling by extracellular matrix-associated Slit/Slit-N maintains fasciculation and position of axon tracts in the nerve cord. PLoS Genet. 13, e1007094.
Bhat, K.M., Gaziova, I., Krishnan, S., 2007. Regulation of axon guidance by slit and netrin signaling in the Drosophila ventral nerve cord. Genetics 176, 2235–2246.
Biteau, B., Jasper, H., 2014. Slit/Robo signaling regulates cell fate decisions in the intestinal stem cell lineage of Drosophila. Cell Rep. 7, 1867–1875.
Blockus, H., Chedotal, A., 2016. Slit-Robo signaling. Development 143, 3037–3044.
Branda, C.S., Stern, M.J., 1999. Cell migration and axon growth cone guidance in Caenorhabditis elegans. Curr. Opin. Genet. Dev. 9, 479–484.
Brankatschk, M., Dickson, B.J., 2006. Netrins guide Drosophila commissural axons at short range. Nat. Neurosci. 9, 188–194.
Brose, K., Tessier-Lavigne, M., 2000. Slit proteins: key regulators of axon guidance, axonal branching, and cell migration. Curr. Opin. Neurobiol. 10, 95–102.
Brose, K., Bland, K.S., Wang, K.H., Arnott, D., Henzel, W., Goodman, C.S., Tessier-Lavigne, M., Kidd, T., 1999. Slit proteins bind Robo receptors and have an evolutionarily conserved role in repulsive axon guidance. Cell 96, 795–806.
Chen, J.H., Wen, L., Dupuis, S., Wu, J.Y., Rao, Y., 2001. The N-terminal leucine-rich regions in Slit are sufficient to repel olfactory bulb axons and subventricular zone neurons. J. Neurosci. 21, 1548–1556.
Chilton, J.K., 2006. Molecular mechanisms of axon guidance. Dev. Biol. 292, 13–24.
Chotard, C., Salecker, I., 2007. Glial cell development and function in the Drosophila visual system. Neuron Glia Biol. 3, 17–25.
Coleman, H.A., Labrador, J.P., Chance, R.K., Bashaw, G.J., 2010. The Adam family metalloprotease Kuzbanian regulates the cleavage of the roundabout receptor to control axon repulsion at the midline. Development 137, 2417–2426.
Contreras, E.G., Palominos, T., Glavic, A., Brand, A.H., Sierralta, J., Oliva, C., 2018. The transcription factor SoxD controls neuronal guidance in the Drosophila visual system. Sci. Rep. 8, 13332.
Contreras, E.G., Sierralta, J., Oliva, C., 2019. Novel strategies for the generation of neuronal diversity: lessons from the fly visual system. Front. Mol. Neurosci. 12, 140.
Cooper, J.A., 2013. Cell biology in neuroscience: mechanisms of cell migration in the nervous system. J. Cell Biol. 202, 725–734.
Delloye-Bourgeois, C., Jacquier, A., Charoy, C., Reynaud, F., Nawabi, H., Thoinet, K., Kindbeiter, K., Yoshida, Y., Zagar, Y., Kong, Y., et al., 2015. PlexinA1 is a new Slit receptor and mediates axon guidance function of Slit C-terminal fragments. Nat. Neurosci. 18, 36–45.
Dominici, C., Moreno-Bravo, J.A., Puiggros, S.R., Rappeneau, Q., Rama, N., Vieugue, P., Bernet, A., Mehlen, P., Chedotal, A., 2017. Floor-plate-derived netrin-1 is dispensable for commissural axon guidance. Nature 545, 350–354.
Edwards, T.N., Nuschke, A.C., Nern, A., Meinertzhagen, I.A., 2012. Organization and metamorphosis of glia in the Drosophila visual system. J. Comp. Neurol. 520, 2067–2085.
Fan, Y., Soller, M., Flister, S., Hollmann, M., Muller, M., Bello, B., Egger, B., White, K., Schafer, M.A., Reichert, H., 2005. The egghead gene is required for compartmentalization in Drosophila optic lobe development. Dev. Biol. 287, 61–73.
Fischbach, K.F., Dittrich, A.P.M., 1989. The optic lobe of Drosophila melanogaster.I. A Golgi analysis of wild-type structure. Cell Tissue Res. 258, 441–475.
Gorostiza, E.A., Colomb, J., Brembs, B., 2016. A decision underlies phototaxis in an insect. Open Biol. 6.
Hao, J.C., Yu, T.W., Fujisawa, K., Culotti, J.G., Gengyo-Ando, K., Mitani, S., Moulder, G., Barstead, R., Tessier-Lavigne, M., Bargmann, C.I., 2001. C. elegans slit acts in midline, dorsal-ventral, and anterior-posterior guidance via the SAX-3/Robo receptor. Neuron 32, 25–38.
Hebrok, M., Reichardt, L.F., 2004. Brain meets pancreas: netrin, an axon guidance molecule, controls epithelial cell migration. Trends Cell Biol. 14, 153–155.
Iwai, Y., Usui, T., Hirano, S., Steward, R., Takeichi, M., Uemura, T., 1997. Axon patterning requires DN-cadherin, a novel neuronal adhesion receptor, in the Drosophila embryonic CNS. Neuron 19, 77–89.
Jen, J.C., Chan, W.M., Bosley, T.M., Wan, J., Carr, J.R., Rub, U., Shattuck, D., Salamon, G., Kudo, L.C., Ou, J., et al., 2004. Mutations in a human ROBO gene disrupt hindbrain axon pathway crossing and morphogenesis. Science 304, 1509–1513.
Kemp, H.A., Cooke, J.E., Moens, C.B., 2009. EphA4 and EfnB2a maintain rhombomere coherence by independently regulating intercalation of progenitor cells in the zebrafish neural keel. Dev. Biol. 327, 313–326.
Kennedy, T.E., Serafini, T., de la Torre, J.R., Tessier-Lavigne, M., 1994. Netrins are diffusible chemotropic factors for commissural axons in the embryonic spinal cord. Cell 78, 425–435.
Kennedy, T.E., Wang, H., Marshall, W., Tessier-Lavigne, M., 2006. Axon guidance by diffusible chemoattractants: a gradient of netrin protein in the developing spinal cord. J. Neurosci. 26, 8866–8874.
Kidd, T., Bland, K.S., Goodman, C.S., 1999. Slit is the midline repellent for the robo receptor in Drosophila. Cell 96, 785–794.
Kiecker, C., Lumsden, A., 2005. Compartments and their boundaries in vertebrate brain development. Nat. Rev. Neurosci. 6, 553–564.
Kraut, R., Zinn, K., 2004. Roundabout 2 regulates migration of sensory neurons by signaling in trans. Curr. Biol. 14, 1319–1329.
Lin, T.Y., Luo, J., Shinomiya, K., Ting, C.Y., Lu, Z., Meinertzhagen, I.A., Lee, C.H., 2016. Mapping chromatic pathways in the Drosophila visual system. J. Comp. Neurol. 524, 213–227.
Long, H., Sabatier, C., Ma, L., Plump, A., Yuan, W., Ornitz, D.M., Tamada, A., Murakami, F., Goodman, C.S., Tessier-Lavigne, M., 2004. Conserved roles for Slit and Robo proteins in midline commissural axon guidance. Neuron 42, 213–223.
Mora, N., Oliva, C., Fiers, M., Ejsmont, R., Soldano, A., Zhang, T.T., Yan, J., Claeys, A., De Geest, N., Hassan, B.A., 2018. A temporal transcriptional switch governs stem cell division, neuronal numbers, and maintenance of differentiation. Dev. Cell 45, 53-66 e55.
Morante, J., Desplan, C., 2008. The color-vision circuit in the medulla of Drosophila. Curr. Biol. 18, 553–565.
Morante, J., Erclik, T., Desplan, C., 2011. Cell migration in Drosophila optic lobe neurons is controlled by eyeless/Pax6. Development 138, 687–693.
Moreno-Bravo, J.A., Roig Puiggros, S., Mehlen, P., Chedotal, A., 2019. Synergistic activity of floor-plate- and ventricular-zone-derived netrin-1 in spinal cord commissural axon guidance. Neuron 101, 625-634 e623.
Neriec, N., Desplan, C., 2016. From the eye to the brain: development of the Drosophila visual system. Curr. Top. Dev. Biol. 116, 247–271.
Ngo, K.T., Andrade, I., Hartenstein, V., 2017. Spatio-temporal pattern of neuronal differentiation in the Drosophila visual system: a user's guide to the dynamic morphology of the developing optic lobe. Dev. Biol. 428, 1–24.
Oliva, C., Choi, C.M., Nicolai, L.J., Mora, N., De Geest, N., Hassan, B.A., 2014. Proper connectivity of Drosophila motion detector neurons requires Atonal function in progenitor cells. Neural Dev. 9, 4.
Oliva, C., Soldano, A., Mora, N., De Geest, N., Claeys, A., Erfurth, M.L., Sierralta, J., Ramaekers, A., Dascenco, D., Ejsmont, R.K., et al., 2016. Regulation of Drosophila brain wiring by neuropil interactions via a slit-robo-RPTP signaling complex. Dev. Cell 39, 267–278.
Ordan, E., Brankatschk, M., Dickson, B., Schnorrer, F., Volk, T., 2015. Slit cleavage is essential for producing an active, stable, non-diffusible short-range signal that guides muscle migration. Development 142, 1431–1436.
Pappu, K.S., Morey, M., Nern, A., Spitzweck, B., Dickson, B.J., Zipursky, S.L., 2011. Robo-3–mediated repulsive interactions guide R8 axons during Drosophila visual system development. Proc. Natl. Acad. Sci. U. S. A. 108, 7571–7576.
Pinto-Teixeira, F., Koo, C., Rossi, A.M., Neriec, N., Bertet, C., Li, X., Del-Valle-Rodriguez, A., Desplan, C., 2018. Development of concurrent retinotopic maps in the fly motion detection circuit. Cell 173, 485-498 e411.
Plazaola-Sasieta, H., Fernandez-Pineda, A., Zhu, Q., Morey, M., 2017. Untangling the wiring of the Drosophila visual system: developmental principles and molecular strategies. J. Neurogenet. 31, 231–249.
Plazaola-Sasieta, H., Zhu, Q., Gaitan-Penas, H., Rios, M., Estevez, R., Morey, M., 2019 Sep 3. Drosophila ClC-a is required in glia of the stem cell niche for proper neurogenesis and wiring of neural circuits. Glia. https://doi.org/10.1002/glia.23691. Epub ahead of print.
Spitzweck, B., Brankatschk, M., Dickson, B.J., 2010. Distinct protein domains and expression patterns confer divergent axon guidance functions for Drosophila Robo receptors. Cell 140, 409–420.
Suzuki, T., Hasegawa, E., Nakai, Y., Kaido, M., Takayama, R., Sato, M., 2016. formation of neuronal circuits by interactions between neuronal populations derived from different origins in the Drosophila visual center. Cell Rep. 15, 499–509.
Suzuki, T., Liu, C., Kato, S., Nishimura, K., Takechi, H., Yasugi, T., Takayama, R., Hakeda-Suzuki, S., Suzuki, T., Sato, M., 2018. Netrin signaling defines the regional border in the Drosophila visual center. iScience 8, 148–160.
Tayler, T.D., Robichaux, M.B., Garrity, P.A., 2004. Compartmentalization of visual centers in the Drosophila brain requires Slit and Robo proteins. Development 131, 5935–5945.
Timofeev, K., Joly, W., Hadjieconomou, D., Salecker, I., 2012. Localized netrins act as positional cues to control layer-specific targeting of photoreceptor axons in Drosophila. Neuron 75, 80–93.
Tsai, H.H., Miller, R.H., 2002. Glial cell migration directed by axon guidance cues. Trends Neurosci. 25, 173–175 discussion 175-176.
Varadarajan, S.G., Kong, J.H., Phan, K.D., Kao, T.J., Panaitof, S.C., Cardin, J., Eltzschig, H., Kania, A., Novitch, B.G., Butler, S.J., 2017. Netrin1 produced by neural progenitors, not floor plate cells, is required for axon guidance in the spinal cord. Neuron 94, 790-799 e793.
Venken, K.J., Schulze, K.L., Haelterman, N.A., Pan, H., He, Y., Evans-Holm, M., Carlson, J.W., Levis, R.W., Spradling, A.C., Hoskins, R.A., et al., 2011. MiMIC: a highly versatile transposon insertion resource for engineering Drosophila melanogaster genes. Nat. Methods 8, 737–743.
Walck-Shannon, E., Hardin, J., 2014. Cell intercalation from top to bottom. Nat. Rev. Mol. Cell Biol. 15, 34–48.
Wallace, K., Liu, T.H., Vaessin, H., 2000. The pan-neural bHLH proteins DEADPAN and ASENSE regulate mitotic activity and cdk inhibitor dacapo expression in the Drosophila larval optic lobes. Genesis 26, 77–85.
Walther, R.F., Pichaud, F., 2006. Immunofluorescent staining and imaging of the pupal and adult Drosophila visual system. Nature Protocols 1 (6), 2635–2642. https://doi.org/10.1038/nprot.2006.379.
Wu, J.S., Luo, L., 2006. A protocol for dissecting Drosophila melanogaster brains for live imaging or immunostaining. Nature Protocols 1 (4), 2110–2115. https://doi.org/10.1038/nprot.2006.336.
Wu, Z., Makihara, S., Yam, P.T., Teo, S., Renier, N., Balekoglu, N., Moreno-Bravo, J.A., Olsen, O., Chedotal, A., Charron, F., et al., 2019. Long-range guidance of spinal commissural axons by Netrin1 and sonic hedgehog from midline floor plate cells. Neuron 101, 635-647 e634.
Yam, P.T., Charron, F., 2013. Signaling mechanisms of non-conventional axon guidance cues: the Shh, BMP and Wnt morphogens. Curr. Opin. Neurobiol. 23, 965–973.
Zou, Y., 2004. Wnt signaling in axon guidance. Trends Neurosci. 27, 528–532.